Deep subwavelength surface modes in metal–dielectric metamaterials

Sung Hyun Nam,[1,3] Erick Ulin-Avila,[1] Guy Bartal,[1] and Xiang Zhang[1,2,*]

[1]*NSF Nanoscale Science and Engineering Center (NSEC), 3112 Etcheverry Hall, University of California, Berkeley, California 94720-1740, USA*

[2]*Materials Sciences Division, Lawrence Berkeley National Laboratory, 1 Cyclotron Road, Berkeley, California 94720, USA*

[3]*Present address, Center for Integrated Nanotechnologies, Materials Physics and Application Division, Los Alamos National Laboratory, Los Alamos, New Mexico 87545, USA*

**Corresponding author: xiang@berkeley.edu*

Received February 11, 2010; revised April 23, 2010; accepted April 28, 2010; posted May 5, 2010 (Doc. ID 124020); published May 24, 2010

We present what we believe to be the first study of deep subwavelength surface modes in binary metal–dielectric metamaterials. By employing anomalous coupling in binary periodicity, peculiar properties of band structure and eigenmode symmetry are obtained. We show that strongly confined plasmonic Tamm-like and Shockley-like surface modes can be formed at the termination of the array. We clarify the character of each surface mode and analyze its unique symmetry with the corresponding band structure.

OCIS codes: 240.6680, 240.6690, 160.3918.

Controlling light dynamics in optical periodic lattices has been actively studied for its fundamental and practical aspects. Recent research on metal–dielectric periodic layers supporting surface plasmon polaritons (SPPs) has shown new possibilities to handle light dynamics such as negative refraction, subwavelength solitons, and focusing [1–5].

Termination of the periodicity brings different properties at the surface from those in the bulk. In condensed matter physics, two types of surface states, Tamm and Shockley states, have been studied, differing in their physical origins and properties [6]: while Tamm states appear due to strong perturbation above a certain threshold at the surface, Shockley states do not require such asymmetry in surface potentials. Shockley states rather arise from crossing of adjacent bands, which requires at least two alternating weak and strong bondings in the lattice and breaking of the strong bonding at the surface. Optical analogues of the surface states also have been studied in photonic lattice systems such as photonic crystals [7,8] and optical waveguide arrays [9–12]. Such optical surface modes have provided new approaches to photon manipulation.

In this Letter, we investigate the novel properties of surface modes in one-dimensional metal–dielectric metamaterials. We demonstrate both Tamm-like and Shockley-like surface modes and study their characteristics. Such surface modes manifest themselves in unique features originating from the anomalous coupling between SPP modes.

We begin by analyzing a binary metal–dielectric metamaterial as an array of single-mode waveguides with alternating coupling coefficients C_+ and C_-, as shown in Fig. 1(a). The alternating coupling is analogous to an s- and p-orbital hybrid atomic chain [6]. It should be noted that the effective medium approach used for simple metal–dielectric structures does not work well for binary metamaterials due to strong internal interactions [13]. Each waveguide [dark gray (blue) bar] is evanescently coupled to its nearest neighbors. The coupling coefficient is defined by $C = (\beta_s - \beta_a)/2$, with β_s and β_a being the propagation constants of the symmetric and antisymmetric modes of two coupled waveguides system, respectively. For index-guided conventional waveguides, the coupling coefficients are always positive. Here we consider a more general case by allowing negative values for the coupling coefficients. The effects of such generalization will be clear below [1,14]. We find the band structure (isofrequency curves) using coupled-mode theory for the field amplitude of the nth waveguide E_n [15]. We express the usual coupled differential equations as more compact Hamiltonian forms:

$$H|\psi\rangle = K|\psi\rangle, \qquad H(\eta,\kappa) = \begin{pmatrix} 0 & \eta e^{-i\kappa} + 1 \\ \eta e^{i\kappa} + 1 & 0 \end{pmatrix}, \qquad |\psi\rangle = \begin{pmatrix} A \\ B \end{pmatrix}. \tag{1}$$

where A and B are the amplitudes of Floquet–Bloch eigenmodes, $a_n = A\exp(i\beta z + i\kappa n)$ for E_{2n} and $b_n = B\exp(i\beta z + i\kappa n)$ for E_{2n+1}, and the eigenvalue $K = (\beta - \beta_0)/C_+$ is the dimensionless propagation constant with β_0 being the propagation constant of the isolated waveguide. The Hamiltonian H is a function of two parameters, $\kappa = k_x\Lambda$ (Λ is the array period) and $\eta = C_-/C_+$ the asymmetry coefficient. From Eq. (1), we obtain two-sheeted isofrequency surfaces $K_\pm(\eta,\kappa) = \pm\sqrt{\eta^2 + 2\eta\cos\kappa + 1}$. Figure 1(b) shows the band structures for positive $\eta = 0.5$ (dotted curves) and negative $\eta = -0.5$ (solid curves). The direct consequence of the negative η is the band inversion: the narrowest bandgap occurs at $\kappa = 0$ and not at $\kappa = \pm\pi$. For the alternating coupling coefficients C_+ and C_-, we have three different combinations of the signs, both positive, both negative, or one positive and one negative. We consider the latter two cases, which are not encountered with conventional dielectric arrays. The K-band structure with all negative coupling coefficients seemingly leads to the same structure as with all positive couplings, since both cases give positive η. They differ in the actual mode symmetry

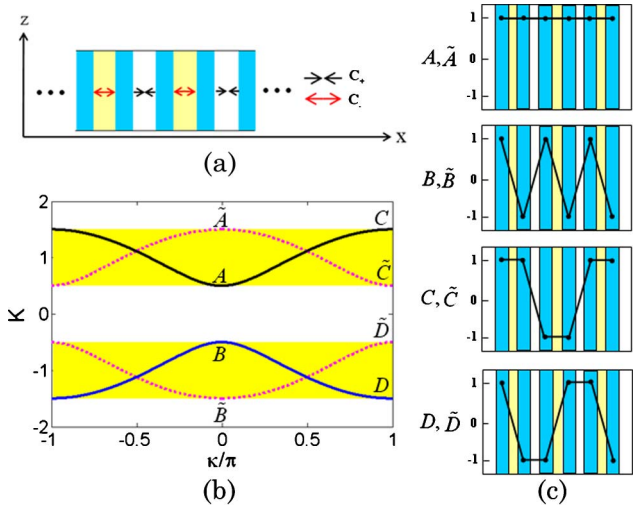

Fig. 1. (Color online) (a) Schematic of 1 – D binary array with alternating coupling C_+ and C_-, dark gray (blue), waveguides, light gray (yellow) and white, coupling regions. (b) Band diagram of dimensionless propagation constant K for asymmetry coefficient $\eta = 0.5$ (dotted curve) and $\eta = -0.5$ (solid curve). (c) Corresponding mode symmetries at the band edges $A - D$ and $\tilde{A} - \tilde{D}$ in (b).

owing to the different sign of C_+ (that is, $\beta = C_+K + \beta_0$). The general and abstract mode symmetries at the edges in K-band are shown in Fig. 1(c).

Such binary arrays are realized by utilizing metal–dielectric layers as seen at the top of Figs. 2(a) and 2(b). The array in Fig. 2(a) consists of metal layers (Au) of alternating thickness (40 nm and 20 nm) and dielectric layers (100 nm, $n = 1.5$) sandwiched by the metal layers.

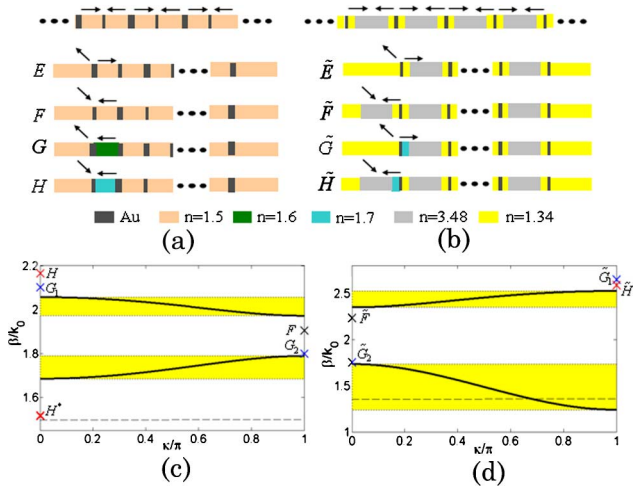

Fig. 2. (Color online) (a), (b) Top, infinite binary metal–dielectric metamaterial; bottom, four types of surface termination at the left end of the array for positive $(E - H)$ and negative $(\tilde{E} - \tilde{H})\eta$, respectively. The arrows indicate strength of the couplings and their breaks: ← →,weak coupling; → ←, strong coupling; ↖ → and ↘←, broken weak and strong couplings, respectively. See the main text for the dimensions. (c), (d) Band structures for the infinite arrays in (a) and (b), respectively. The corresponding β for each surface mode in (a) and (b) are also marked in the diagrams. The dashed lines in the figures indicate the refractive index of the external layer (not isofrequency curves), $n_{\text{ext}} = 1.5$ and $n_{\text{ext}} = 1.34$, respectively. The type E and $\tilde{E}$ do not support surface modes.

The operating wavelength is 1550 nm. The gap SPP modes confined in each dielectric layer are coupled through the metal layers. In such a case, negative permittivity of the metal results in negative sign of the coupling coefficient [1]. Thus, two coupling coefficients of the array in Fig. 2(a) are both negative ($C_- < C_+ < 0$) with alternating weak (C_+, through 40 nm) and strong (C_-, through 20 nm) coupling strength. On the other hand, the array in Fig. 2(b) has one positive ($C_+ > 0$) and one negative ($C_- < 0$) coefficient. The unit cell consists of metal (20 nm, Au), low-index (50 nm, $n = 1.34$), high-index (200 nm, $n = 3.48$), and another low-index dielectric (50 nm, $n = 1.34$) layers consecutively. For a single unit cell with infinite thickness of the outer layers, the mode is highly confined in the 50 nm low-index layer forming a hybrid SPP mode [16]. The thicknesses of the low- and high-index layers are chosen to allow only single mode. The normal and anomalous couplings occur through the silicon and the metal layers, respectively. The band structures for the two infinite arrays are calculated by transfer matrix method [17] with the Drude permittivity of gold [18]. The results are shown in Figs. 2(c) and 2(d). The band of each array exhibits opposite curvature from each other. The notable asymmetry of the upper and lower band and the large band broadening are attributed to the strong coupling between the modes.

Now let us turn to the formation of the surface modes by considering finite arrays of 20 unit cells for each type of array in Figs. 2(a) and 2(b). The finite arrays can have

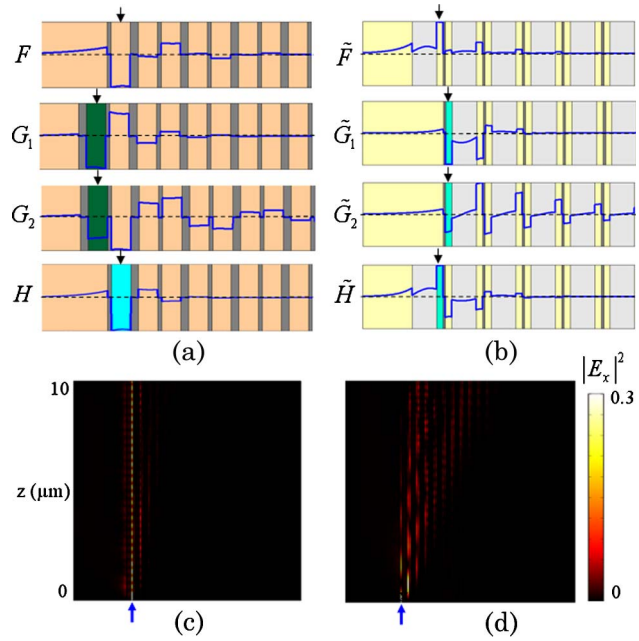

Fig. 3. (Color online) (a), (b) Mode field profile (E_x) for each surface mode $F \sim H$ and $\tilde{F} \sim \tilde{H}$ in Fig. 2, respectively. The fields are normalized to the maximum. The arrows indicate the surface waveguides. The decay length of each surface mode is 4.2, 3.1, 8.0, and 3.5 μm for F, G_1, G_2, and H, respectively and 14.4, 7.6, 2.7, and 5.1 μm for $\tilde{F}$, $\tilde{G}_1$, $\tilde{G}_2$, and $\tilde{H}$, respectively. (c), (d) Propagation of the Shockley-like surface mode (type $\tilde{F}$) and the extended state (type $\tilde{E}$ in Fig. 2), respectively. Only the surface waveguide at the left end is excited (arrows). The electric field intensity is normalized to the maximum. The color code range is set to 0–0.3, and the metal loss was artificially reduced for the better visibility of propagation.

four different types of lattice termination ($E-H$ and $\tilde{E}-\tilde{H}$), depending on the presence of the perturbations and which coupling breaks. The termination at the left ends may support localized surface modes. The right ends are "passivated" with a break of the weak coupling, which minimizes its effects on the left ends. Here we focus on the surface modes at the left end surface. The interaction between two end surfaces in a finite array will be addressed elsewhere. The termination types E ($\tilde{E}$) and F ($\tilde{F}$) correspond to a break of the weak and the strong coupling, respectively, with no additional surface perturbation. On the other hand, the termination types G ($\tilde{G}$) and H ($\tilde{H}$) represent a break of the weak and the strong coupling, respectively, with strong surface perturbation. The surface perturbation is made by increasing the refractive indices of the surface waveguides. We find the discrete eigenvalues (β/k_0) for each type of surface termination, and those are marked in the band diagrams in Figs. 2(c) and 2(d). Being consistent with the surface states in solids, the type E ($\tilde{E}$) does not support any surface modes owing to the break of the weak coupling and no surface perturbation. The type F ($\tilde{F}$) supports a localized mode even without surface perturbation, which is the characteristic of Shockley-like surface modes and is attributed to the break of the strong coupling. As seen in Fig. 2, the Shockley-like modes (F and $\tilde{F}$) are located within the center bandgap. Strong surface perturbations can induce Tamm-like localized modes regardless of which coupling breaks, which are exemplified with the type G ($\tilde{G}$) and H ($\tilde{H}$). The type G ($\tilde{G}$) Tamm-like modes can have two eigenvalues, one either above or below the band edges (G_1, $\tilde{G}_1$) and the other one within the center bandgap (G_2, $\tilde{G}_2$). For the type H ($\tilde{H}$), it would be the type F ($\tilde{F}$) Shockley-like mode if there were no surface perturbation. With a strong perturbation, the eigenvalue moves to above (with increased refractive index) or below the band edges from the center bandgap, which makes its character identified as Tamm-like mode [19].

A major difference between the surface modes in the positive η arrays and those in negative η arrays is their mode symmetries due to the opposite band curvatures. This becomes clear in Figs. 3(a) and 3(b), where the mode fields (E_x) for each type of surface mode are plotted. The mode fields are highly localized in the surface waveguides and decay into the bulk. The decay rate depends on how close the eigenvalue β is to the band edges. The closer, the slower the decay rate is. All the mode profiles resemble the modes at nearby band edges [see Fig. 1(c)]. For the Shockley-like modes F and $\tilde{F}$, the fields are mostly confined in the odd-numbered waveguides. The type F mode has alternating sign at every odd-numbered waveguide, while the type $\tilde{F}$ mode keeps the same sign, which approximates the sum of the modes at the band edges $\tilde{C}-\tilde{D}$, and $A-B$ in Fig. 1(c), respectively. The Tamm-like modes G_1 and H in the positive η array are located above the upper band edge and change their field sign at every adjacent waveguide, since the propagation constant of the antisymmetric mode is bigger than that of the symmetric mode for the anomalous coupling. The Tamm-like modes $\tilde{G}_1$ and $\tilde{H}$ in the negative η array change their field signs at every other waveguide because of the alternating normal and anomalous couplings. For another Tamm-like modes G_2 and $\tilde{G}_2$ located within the center bandgap, their fields are confined more in the even-numbered waveguides unlike the Shockley-like modes. We also calculate the decay length, $L = 1/(2\mathrm{Im}(\beta))$ of each surface mode (see the figure caption). All-antisymmetric modes such as G_1, H, and $\tilde{G}_2$ have shorter decay lengths compared with others, and all-symmetric mode $\tilde{F}$ has the longest decay length. We confirm the formation of the surface modes by numerically demonstrating their propagation using a finite-element method. The propagation of the Shockley-like surface mode (type $\tilde{F}$) and the extended mode (type $\tilde{E}$) are shown in Figs. 3(c) and 3(d), respectively. Only the surface waveguide at the left end is excited. It is clearly seen that while the extended mode $\tilde{E}$ penetrates into the bulk, the Shockley-like surface mode $\tilde{F}$ remains localized at the surface.

To summarize, we have theoretically demonstrated deeply confined subwavelength surface modes supported in binary metal–dielectric metamaterials. We have identified the character of each surface mode and provided a scheme for experimental realization.

This work has been supported by U.S. Army Research Office (ARO) MURI program 50432 PH-MUR, and by the NSF Nano-scale Science and Engineering Center (NSEC) under grant CMMI-0751621.

References and Notes

1. X. Fan, G. P. Wang, J. C. W. Lee, and C. T. Chan, Phys. Rev. Lett. **97**, 073901 (2006).
2. Y. Liu, G. Bartal, D. A. Genov, and X. Zhang, Phys. Rev. Lett. **99**, 153901 (2007).
3. L. Verslegers, P. B. Catrysse, Z. Yu, and S. Fan, Phys. Rev. Lett. **103**, 033902 (2009).
4. G. Bartal, G. Lerosey, and X. Zhang, Phys. Rev. B **79**, 201103 (R) (2009).
5. S. Feng, J. M. Elson, and P. L. Overfelt, Opt. Express **13**, 4113 (2005).
6. S. G. Davison and M. Steslicka, *Basic Theory of Surface States* (Oxford Univ. Press, 1996).
7. N. Malkova and C. Z. Ning, Phys. Rev. B **73**, 113113 (2006).
8. K. Ishizaki and S. Noda, Nature **460**, 367 (2009).
9. P. Yeh, A. Yariv, and A. Y. Cho, Appl. Phys. Lett. **32** 104(1978).
10. M. I. Molina, I. L. Garanovich, A. A. Sukhorukov, and Y. S. Kivshar, Opt. Lett. **31**, 2332 (2006).
11. I. L. Garanovich, A. A. Sukhorukov, and Y. S. Kivshar, Phys. Rev. Lett. **100**, 203904 (2008).
12. N. Malkova, I. Hromada, X. Wang, G. Bryant, and Z. Chen, Phys. Rev. A **80**, 043806 (2009).
13. J. Yang, X. Hu, X. Li, Z. Liu, X. Jiang, and J. Zi, Opt. Lett. **35**, 16 (2010).
14. A. Locatelli, M. Conforti, D. Modotto, and C. D. Angelis, Opt. Lett. **30**, 2894 (2005).
15. A. A. Sukhorukov and Y. S. Kivshar, Opt. Lett. **27**, 2112 (2002).
16. R. F. Oulton, V. J. Sorger, D. A. Genov, D. F. P. Pile, and X. Zhang, Nat. Photonics **2**, 496 (2008).
17. P. Yeh, *Optical Waves in Layered Media* (Wiley, 1988).
18. $\varepsilon_{Au} = \varepsilon_\infty - \omega_p^2/\omega(\omega + i\gamma_c)$ where $\varepsilon_\infty = 10$, $\omega_p = 1.4 \times 10^{16}$, and $\gamma_c = 1.1 \times 10^{14}$.
19. The two eigenvalues for the type H near $\beta/k_0 = 1.5$ in Fig. 2(c) have different physical origins. One is single interface SPP-like mode on the leftmost metal surface, and the other one is associated with a localized mode on the right end due to the strong interaction. Those modes are not the surface modes of interest in this Letter.